Progress In Electromagnetics Research, Vol. 110, 179–197, 2010

TRANSIENT TIME-DEPENDENT ELECTRIC FIELD OF DIELECTRIC BODIES USING THE VOLTERRA INTEGRAL EQUATION IN THREE DIMENSIONS

A. Al-Jarro, P. Sewell, T. M. Benson, A. Vukovic, and J. Paul

George Green Institute for Electromagnetics Research
Electrical Systems and Optics Research Division
Faculty of Engineering, The University of Nottingham
University Park, Nottingham, NG7 2RD, UK

Abstract—An accurate and flexible three-dimensional Volterra Time Domain Integral Equation (TDIE) algorithm is presented and implemented here to model the time-dependent electromagnetic field of arbitrarily shaped dielectric bodies. This development is motivated by the need for a modern high-resolution numerical tool that is capable of providing a full and comprehensive investigation of devices containing a diverse range of feature sizes or boundaries, in all three space dimensions plus time. Stability, accuracy and convergence of the algorithm are discussed and verified by means of canonical working examples.

1. INTRODUCTION

This paper presents a volume time domain integral equation based technique for studying the transient time-dependent electric field of three-dimensional dielectric bodies having arbitrary shapes. The ability to accurately and cost-effectively simulate electromagnetic wave interactions with penetrable bodies containing a diverse range of feature sizes having boundaries that are curved or non-tangential to the coordinate axes of complex and/or time varying material response is of significant practical interest for many applications in photonics and optoelectronics [1, 2]. Other important areas of interest including broadband response, optical behaviour, identification, bioelectromagnetic applications [3], imaging and chemical identification processes [4].

Received 23 September 2010, Accepted 28 October 2010, Scheduled 18 November 2010
Corresponding author: Ahmed Al-Jarro (ahmed.aljarro@nottingham.ac.uk).

To this effect, and over the recent years, corresponding electromagnetic investigations have drawn increasing attention in the scientific community due to continuing theoretical and technological developments in this discipline. Simultaneously, a similar advancement, with the wide availability of high speed computers, has provided reliable design and analysis tools for their examination. Typically, these interactions can be analyzed using methods that are based on the differential or integral form of the Maxwell equations. Common volumetric differential equations techniques include finite difference time domain (FDTD) [5], transmission line modelling (TLM) [6], and finite volume time domain (FVTD) [7]. The primary drawback of these methods is i) they require discretization of the full problem space and ii) the need to artificially impose radiation conditions. In contrast, solutions to electromagnetic problems obtained using time domain integral equations (TDIE) schemes only i) require the direct discretization of regions whose material properties differ from a background material and ii) inherently satisfy radiation conditions; therefore eliminating this potential source of error when explicitly constructing absorbing or perfectly matched boundary conditions. However, in the past, time domain integral equation based methods were often found to be computationally expensive compared to their differential equation based counterparts, and suffer from late time instability in the form of high frequency oscillation [8–10]. Recently the efficiency of TDIE techniques has increased dramatically with the advent of acceleration schemes such as the plane wave time domain algorithm [11] and the fast Fourier transform accelerated schemes [12]. Furthermore, the marching-on-in-time methods for solving TDIE, that have been shown prone to late time instabilities, have also been successfully treated for various scenarios through the use of spatial and/or temporal filtering techniques [13–16], and the implementation of accurate spatial interpolation rules with implicit time-stepping schemes [17–20]. In addition, a backward finite difference approximation, resulting in an implicit technique, to minimise these late-time oscillations has also been proposed [21, 22]. However, evidently this should be used with care, due to the damping properties of the backward Euler which can affect the solution accuracy.

It is also noted that the choice of a particular TDIE method depends on the nature of the problem under consideration. Whereas for penetrable homogeneous media, surface integral equation schemes [23–25] are the most appropriate; volume integral equation methods are more suitable when the structure is inhomogeneous [26]. While continuous effort has been employed to further advance numerical techniques involving volume integral equations in the frequency domain for various applications [27–32], to our knowledge, limited progress

has been reported in the time domain [26, 33]. In these schemes, the solution of the problem is often based on employing well established techniques such as the finite element (FE) method [28] and method of moment (MoM) [34]. For such scenarios, the integral equation is discretized and represented by a set of basis functions that leads to systems with fully populated matrices, which is found to impose large memory requirement [31]. Numerical methods are then employed to solve these matrices, where they are often required to undergo additional mathematical conditioning or specific numerical treatment in order to obtain the solution successfully [28, 34]. Commonly applied algorithms for this purpose are either based on conjugate gradient type methods [35] which search for the solution iteratively and/or error minimization of the formulation, formally known as Galerkin testing, [27].

Alternatively, the nodal field sample values can be evaluated in an evolutionary manner, first pioneered by Nerukh et al. [36–38], and also reported in our previous work for the one-dimensional (1D) [39–42] and three-dimensional (3D) [43, 44] cases. To date, successful investigation of the Volterra TDIE has been demonstrated for the 1D case for various scenarios; illustrating their ability to consider nonlinear, dispersive and plasma-like materials as well as to deal with problems in which the material properties are varying in time [40, 41]. Furthermore, their solution has also been demonstrated on modified rectangular space-time meshes [40], and on unstructured triangular space-time meshes [42]. These simple modifications were found to radically increase the flexibility of the computer implementations of the algorithm, allowing numerical solutions that are both stable and accurate for various media without any reservation on the structure geometry, meshing requirements or permittivity contrast between the discontinuity region and background media. Nevertheless, the 3D scenarios have not been thoroughly studied. In this work we progress on such a scheme; providing a detailed investigation of their algorithmic development, and in particular, for the specific case where the geometrical description of the problem under investigation is approximated using cubical building blocks for their simulation. Nevertheless, a Volterra TDIE scheme capable of running on unstructured tetrahedral meshes has already been reported by the authors in [43, 44]; where a full and complete characterization of their algorithmic implementation, along the lines presented in this work, is to appear in a subsequent publication.

As aforementioned, almost all marching-on-in-time numerical solutions for the time domain integral equations based schemes suffer from late time instabilities [13–20]. This is also reported for some

of the differential based methods, such as the FDTD [45]. While in the cases of MoM and FE approaches, compensatory numerical treatment has focused on a combination of careful design and choice of spatial and temporal basis functions and the use of filtering techniques, nevertheless, complete removal of these late time oscillations has met with limited success in the general case. Consequently, it is still often required that special attention must be given to the geometry of the structure, its physical parameters and the mesh used. It is no exception that this phenomenon is also observed when using the Volterra TDIE based schemes, as reported in our previous work [40, 44]. While in the 1D case, numerical instabilities were completely eliminated from their earlier implementations [39] by means of both a semi-implicit formulation and a central difference Crank-Nicholson technique [40]; for the 3D case, a more general treatment of such phenomena is needed. This is shown here to be achieved by employing a low pass digital filtering technique [15], also known as an averaging scheme. In this approach, the values of a small number of previous field values are required at any given moment in time in order to stabilize the computations; therefore incurring an additional but limited computational effort for a successful and complete elimination of the instabilities as illustrated in Section 3.

The development of a novel 3D Volterra time domain integral equation algorithm capable of running on arbitrarily shaped volumetric meshes is presented here. In section 2, the general algorithmic formulation is derived for their solution. In Section 3, we apply this general formalism to model the more specific structures in order to assess stability, accuracy and convergence of the proposed scheme.

2. THEORY

In general, the electric field for a 3D volumetric structure satisfies a Volterra integral equation [36–38],

$$\mathbf{E}(t,r) = \mathbf{E}_o(t,r) + \frac{1}{\varepsilon_b \varepsilon_o} \int_0^t dt' \int_V dr' \left[\frac{1}{4\pi} \left(\nabla\nabla\cdot - \frac{\partial^2}{v^2 \partial t^2} \right) \frac{\delta\left(R/v - (t-t')\right)}{R} \right] \times \left[\mathbf{P}(t',r') - (\varepsilon_b - 1)\varepsilon_o \mathbf{E}(t',r') \right] \quad (1)$$

where ε_b and v are the relative permittivity and speed of light in the background medium. $\mathbf{P}$ is the polarisation of the media, $\mathbf{E}_o$ is the excitation field, t and $r = (x, y, z)$ denote the time and space coordinates, r is the observation point and r' is a source point, $R = |r - r'|$ denotes distance from the source location to the observer

location and t', the temporal integral parameter, runs over the time history, i.e., $0 \leq t' \leq t$.

It is noted that the domain of the spatial integration only encompasses the discontinuity, i.e., the region whose properties differ from the background medium, here taken to lie $r \in V$, re-iterates a significant advantage of this approach compared to the differential equations based numerical methods where full discretization of the problem space is required. Similarly, there is no need to terminate the calculation window with artificial absorbers as the kernel of the integral equation intrinsically contains the correct asymptotic behaviour at infinity.

The equations are based upon generalized functions and are convenient for investigating electromagnetic transients, especially those with moving wave fronts and involving an arbitrary time-spatial dependence of the medium parameters, such as plasmas, semiconductors, non-linear dielectrics and dissipative media. In principle these modifications can be implemented by merely redefining the functions describing the incident field or the medium polarization [36–41]. At each instant of time, the present electric field in (1) is determined via a four-dimensional integral over the space-time history of the field. However, this is immediately reduced to a 3D integral due to the properties of the delta function. Namely, the integral in (1) exists when the argument of the delta function is zero, i.e., $t' = t - R/v$, as illustrated in (2), yielding a process which is visualized as integrating over the surface of spheres of the time-retarded field values.

$$\mathbf{E}(t,r) = \mathbf{E}_o(t,r) + \left(\nabla\nabla\cdot - \frac{\partial^2}{v^2\partial t^2}\right)\frac{1}{\varepsilon_b\varepsilon_o}\frac{1}{4\pi}\int\limits_V dr'\left[\frac{[\mathbf{P}(t',r') - (\varepsilon_b - 1)\varepsilon_o\mathbf{E}(t',r')]}{R}\right] \quad (2)$$

At each instant in time and space the integrand in (2) is evaluated first before applying the Green's tensor $\nabla\nabla\cdot - \partial^2/v^2\partial t^2$. In the development of TDIE approach, structures are subdivided into an adequate number of small sub-volume elements e. The sampling 3D field points are then specified to fall at the centre of mass of each element, where the corresponding nodal field values are assumed constant. These elemental sub-volumes then evolve in time with a fixed time step size allowing for signal propagation in time. For simplicity let

$$\mathbf{F}(t,r) = \frac{1}{\varepsilon_b\varepsilon_o}\frac{1}{4\pi}\int\limits_V dr'\left[\frac{[\mathbf{P}(t',r') - (\varepsilon_b - 1)\varepsilon_o\mathbf{E}(t',r')]}{|r - r'|}\right]. \quad (3)$$

The integration in (3) runs over the entire discontinuity scatterer volume V, and algorithmically reduces to a simple and straightforward summation given by

$$\mathbf{F}(N_t\Delta t, r_i) = \frac{1}{\varepsilon_b\varepsilon_o}\frac{1}{4\pi}\sum_{i\neq j}^{N_e} V_j \left[\frac{[\mathbf{P}(T', r_j) - (\varepsilon_b - 1)\varepsilon_o\mathbf{E}(T', r_j)]}{|r_i - r_j|}\right] + \frac{1}{\varepsilon_b\varepsilon_o}\frac{1}{4\pi}\left[\mathbf{P}(N_t\Delta t, r_i) - (\varepsilon_b - 1)\varepsilon_o\mathbf{E}(N_t\Delta t, r_i)\right]\int \frac{1}{R_{Sing_{i=j}}}, \quad (4)$$

where N_e is the number of elements e within the scatterer V, V_j is the element volume, N_t is the number of time steps, Δt is the time step size, $r_i = (x_j,\ y_j,\ z_j)$ and $r_j = (x_j,\ y_j,\ z_j)$ are the location of observation and source points respectively. The retarded time $T = N_t\Delta t - |r_i - r_j|/v$, such that $0 \leq i,\ j \leq N_e$. It is observed that the expression in (4) diverges for $i = j$. Therefore whenever both the observation point, r_i, and source point, r_j, are inside the scatterer V, the principal value must be taken for the integral in (3) and the singularity of the Green's tensor treated analytically. Algorithmically, the corresponding value of this singular region coincide with, $\mathbf{E}(N_t\Delta t, r_i)$, the unknown nodal field value currently being evaluated and therefore is transformed to the left hand side of (2). For an arbitrary volumetric region containing $R_{Singi=j}$ the corresponding analytical solution is obtained using the analysis described in [46], for a polyhedron, whereas for the specific rectangular case, the more simplified approach for a cube is detailed in [47]. Note that only one singular point is associated with each sub-volume, element, within the scatterer region, V, and therefore needs only be calculated once for the entire problem, as a pre-processing step.

It is important to note that the numerical advantages in evaluating the summation in (4) prior to the application of the Green tensor; not only does it reduce the computational expense significantly, but it also enforces the correct algorithmic interpretation of the mathematical formulations in (1) and therefore satisfies the precise physical behaviour of the problem under investigation. In addition, while evaluating (4); an interpolating technique is performed in order to obtain the time retarded field values that fall in between the surfaces of the spheres of integration from the already calculated nodal field values on the uniform time mesh. Therefore, a simple linear interpolation scheme, in time, is adopted here, such that whenever the value of $T' = N_t\Delta t - |r_i - r_j|/v$ is not an integer multiple of Δt, the corresponding value of $\mathbf{E}(T', r_j)$ is obtained by applying

$$\mathbf{E}(N_t\Delta t + \alpha, r_i) = (1 - \alpha)\mathbf{E}(N_t\Delta t, r_i) + \alpha\,\mathbf{E}(N_t\Delta t + \Delta t, r_i), \quad (5)$$

where $0 \leq \alpha \leq 1$. Substituting for (4) into (2) gives

$$\mathbf{E}(N_t\Delta t, r_i) = \mathbf{E}_o(N_t\Delta t, r_i) + \left(\nabla\nabla\cdot - \frac{\partial^2}{v^2\partial t^2} \right) \mathbf{F}(N_t\Delta t, r_i) \quad (6)$$

The Green's tensor, involving the time and space derivative operators in (6) is discretized using simple and straightforward finite difference techniques. From first inspection, the term involving the second-order time derivatives can be approximated using central difference formula such that

$$\frac{\partial^2\mathbf{F}}{\partial t^2} \approx \frac{\mathbf{F}_+(N_t\Delta t+\Delta t, r_i) - 2\mathbf{F}_o(N_t\Delta t, r_i)+\mathbf{F}_-(N_t\Delta t-\Delta t, r_i)}{\Delta t^2}. \quad (7a)$$

Three consecutive values of $\mathbf{F}$ are therefore required at a given moment in time, i.e., at $\mathbf{F}_+$, $\mathbf{F}_o$ and $\mathbf{F}_-$. However, in order to satisfy causality condition, special attention must be given whenever the distance between the observer and a source region does not satisfy the relation $T^{'} \leq N_t\Delta t - 2\Delta t$. In this case, the central difference approximation for the time derivative in (7a) is replaced by a backward difference scheme given by (7b); therefore ensuring an overall implicit scheme.

$$\frac{\partial^2\mathbf{F}}{\partial t^2} \approx \frac{\mathbf{F}_+(N_t\Delta t, r_i)-2\mathbf{F}_o(N_t\Delta t-\Delta t, r_i)+\mathbf{F}_-(N_t\Delta t-2\Delta t, r_i)}{\Delta t^2} \quad (7b)$$

The spatial derivatives involving the $\nabla\nabla\cdot$ term are then evaluated in a straightforward manner; such that, for example an un-mixed second order derivative is approximated using

$$\frac{\partial^2\mathbf{F}}{\partial y^2} \approx \frac{\mathbf{F}_o(x_i, y_i+\Delta y, r_i) - 2\mathbf{F}_o(x_i, y_i, r_i) + \mathbf{F}_o(x_i, y_i-\Delta y, r_i)}{\Delta y^2}, \quad (8a)$$

and for a mixed second order derivative it is approximated as

$$\frac{\partial^2\mathbf{F}}{\partial x\partial y} \approx \frac{\left[\begin{array}{c} \mathbf{F}_o(x_i+\Delta x, y_i+\Delta y, z_i)-\mathbf{F}_o(x_i+\Delta x, y_i-\Delta y, z_i) \\ -\mathbf{F}_o(x_i-\Delta x, y_i+\Delta y, z_i)+\mathbf{F}_o(x_i-\Delta x, y_i-\Delta y, z_i) \end{array}\right]}{4\Delta x\Delta y}. \quad (8b)$$

In this work, the generality of the algorithm is demonstrated by evaluating the discretized field values on a rectangular volumetric grid for the Volterra TDIE algorithm. The choice of spatial mesh size is dictated by the need to sufficiently and accurately sample the field behaviour in the structure; and as a result, the choice of the time step size, Δt, is dictated by the Courant condition, $\Delta t <= r_{\min}/v$, of the underlying mesh. Here, $r_{\min}$ denotes the shortest distance between any two centroids of all elements populating the scatterer region, V.

Stability, accuracy and convergence of the algorithm are discussed and verified by means of canonical working examples as illustrated

in Section 3. In all cases a changed dielectric media is introduced in an otherwise uniform background medium at zero moment in time. In theory, the background medium can be of any homogeneous linear non-dissipative material and is chosen here to be free space for convenience. The material considered within the discontinuity region can also be linear, non-linear, dissipative, frequency dependent and/or a combination of them [36–40], however, for simplicity it is considered here to be linear, isotropic and nondissipative of relative permittivity ε_1. For this case, the associated polarization function is defined by

$$\mathbf{P}(t', r') = (\varepsilon_1 - 1)\varepsilon_o \mathbf{E}(t', r'). \tag{9}$$

where ε_1 is the relative permittivity constant within the scatterer region, V.

3. NUMERICAL RESULTS

In this section, the Volterra TDIE scheme is applied to several penetrable bodies in order to assess the stability, accuracy and convergence of the algorithm outlined in Section 2. This is verified in three steps. First, a dielectric cube is considered where the generality of the algorithm is tested. The simulated results are compared with those obtained from a differential equation based scheme; with focus on drawing the necessary guidelines required in order to ensure stability of the Volterra TDIE algorithm. In this case, the comparison is carried out with results generated from simulating identical structures using our in house built TLM solver [48]. Second, the accuracy of the proposed Volterra TDIE scheme is verified on three-dimensional structures where analytic solution of the transient time-dependent electric field is available. A dielectric microsphere is therefore considered next, where the time-dependent response of the input signal is compared with the analytically obtained solution using Mie series [49]. Third, more general cases are considered; including a cylinder and a cone. Although unstructured meshes are more suited for modelling the latter scenarios, for apparent reasons [43, 44]; here the rectangular structured grids are considered in order to demonstrate the validity of the proposed scheme against the TLM scheme, which uses cubical building blocks.

The incident field used in all examples that follow is chosen to be a pulse that is a Gaussian function in space and time. The field propagates in the x-direction and the pulsed plane wave is polarized in the normal y-direction, $\hat{\mathbf{y}}$, such that

$$\mathbf{E}_o(N_t\Delta t, r_i) = \hat{\mathbf{y}} \exp\left[\ln(s)\left(N_t\Delta t - t_o - x_i/v\right)^2/h^2\right]. \tag{10}$$

In (10), $s = 0.001$ is the truncation amplitude, h is the temporal pulse half width and t_o is the time delay. In each example, the relative permittivity constant, ε_1, of the scatterer is chosen to be $1.96\varepsilon_b$, with guidance to define the mesh within the scatterer so that there are approximately 10 spatial unknowns per wavelength at the maximum frequency, $f_{\max}$, of the input signal within the dielectric medium.

3.1. Stability

In the first example, a plane wave is normally incident on a face of a dielectric cube having a side length of 0.55 μm, as shown in Fig. 1. The parameters chosen for the incident pulse in (10) are $t_o = 2.0$ fs and $h = 2.0$ fs. A structured rectangular grid description of the cubic geometry is used in this example, testing for the stability of the proposed algorithm, given by (6). A spatial step size of $\Delta x = 0.025$ μm is used for validation, yielding a discretized mesh of $N_e = 10648$ elements within the dielectric cube.

Figure 1 shows a typical result which was obtained by direct application of (6). The transient time-dependent electric field at the centre of the dielectric cube is plotted. Two illuminations are considered; the solid line is that of the above Gaussian pulse and the broken line is when this excitation is applied only for the first time step. The objective is to demonstrate the exponentially growing behaviour of the late time response and also to show that these instabilities are in fact present from the beginning of the solution as it is stepping in time. It is observed that these instabilities are usually small compared

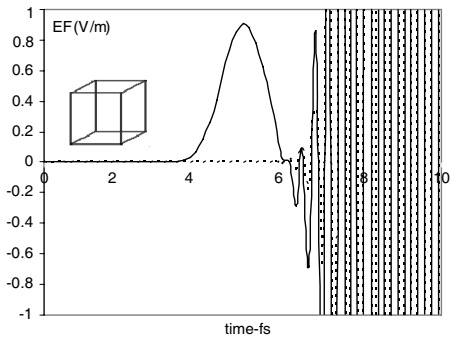

Figure 1. Electric field at the centre of a dielectric cube of side length 0.55 μm. Gaussian pulse excitation, in solid line, and excitation only for one time step, in dotted line. Note that instabilities are present almost from the beginning of the simulation.

to the true solution until later times, when they form the dominant part of the solution. It is reiterated that these instabilities are also observed and treated for most of the time-domain integral methods, as discussed in. In order to eliminate this source of numerical instability, a finite impulse response low pass digital filtering technique, FIR-LPF, [15], also known as an averaging scheme is implemented here; where the underlying concept is simply a de-correlation of accumulated computational noise. The filter is designed and numerically implemented in such a way to eliminate the chances of parasitic sinusoids, whose frequencies are outside the spectrum of excitation and have the potential to grow exponentially [50]. Following the steps outlined in [45], the Kaiser window filter design method results in $[-0.00921971, -0.0466512, 0.257662, 0.600069, 0.257662, 0.0466512, -0.00921971]$ as the impulse response for the seven-element FIR-LPF used for this example.

Figure 2 shows the normalized DFT of the excitation Gaussian pulse used in the example of Fig. 1, in dotted line, and the corresponding normalized DFT response of the FIR-LPF used here, in solid line. It is observed that the bandwidth of the excitation (and therefore the response) is much less than the bandwidth of the filter. Hence we expect that application of this filtering technique will not have a noticeable effect on the computed electric field. The reader is referred to [15] for a detailed analysis of the filter implementation within the numerical algorithm. The proposed method is referred to as the Volterra time domain integral equation, VTDIE, in Figs. 3–6. Fig. 3 demonstrates the results of applying the above filter to the problem of Fig. 1.

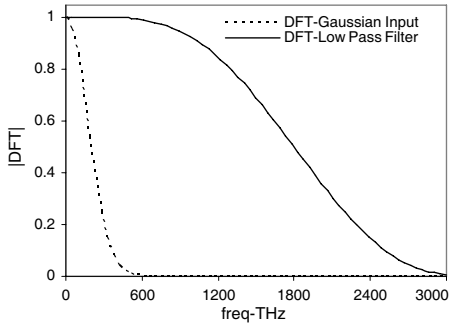

Figure 2. Normalized Discrete Fourier Transform (DFT) of the excitation Gaussian pulse used in the example of Fig. 1, in dotted line, and normalized frequency response of the seven-element digital filter, in solid line.

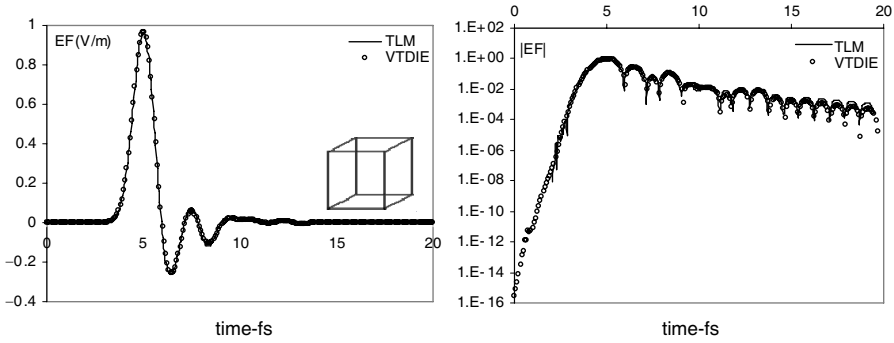

Figure 3. Electric field at the centre of the dielectric cube considered in problem Fig. 1. Proposed method using the finite impulse response lowpass filter, in circles, and the corresponding TLM results generated form simulating an identical input, in solid line. In both methods, a spatial step size $\Delta x = 0.025\,\mu$m, yielding a total number of elements (cells) $N_e = 10648$ are used. (a) Linear scale. (b) Logarithmic scale.

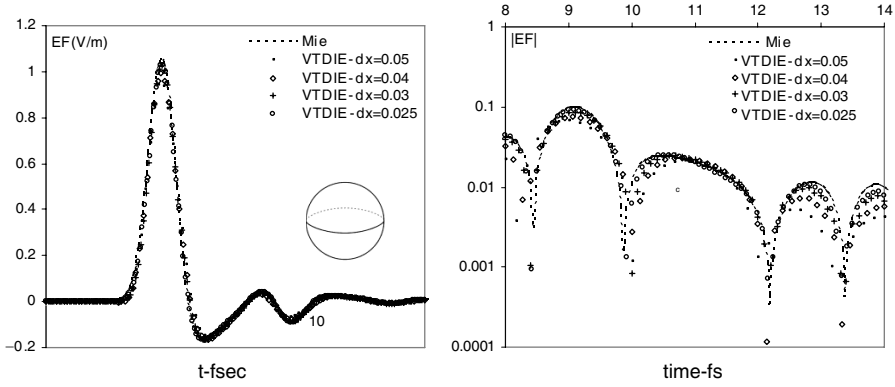

Figure 4. Electric field at the centre of the dielectric microsphere. VTDIE method for various step sizes demonstrating convergence of the proposed algorithm and the corresponding analytic Mie series solution, in dotted line. (a) Linear scale. (b) Logarithmic scale.

It is observed that the instabilities are completely eliminated and they do not show a tendency of appearing in the late times. Also shown in Fig. 3, the transmission line modelling, TLM, method results for an identical problem with the same number of elements

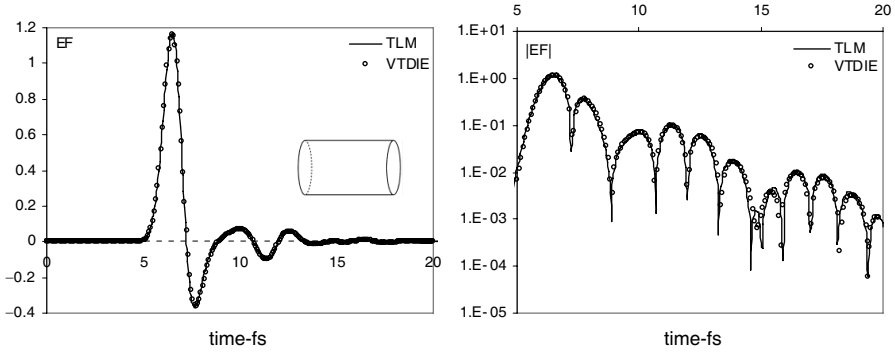

Figure 5. Electric field at the centre of the dielectric cylinder with base radius $a = 0.25\,\mu\text{m}$ and a height $h = 1.0\,\mu\text{m}$. VTDIE, in circles, and the corresponding TLM results generated form simulating an identical structure and input, in solid line. In both methods, a spatial step size $\Delta x = 0.025$, yielding a total number of elements (cells) N_e=12200 is used. (a) Linear scale. (b) Logarithmic scale.

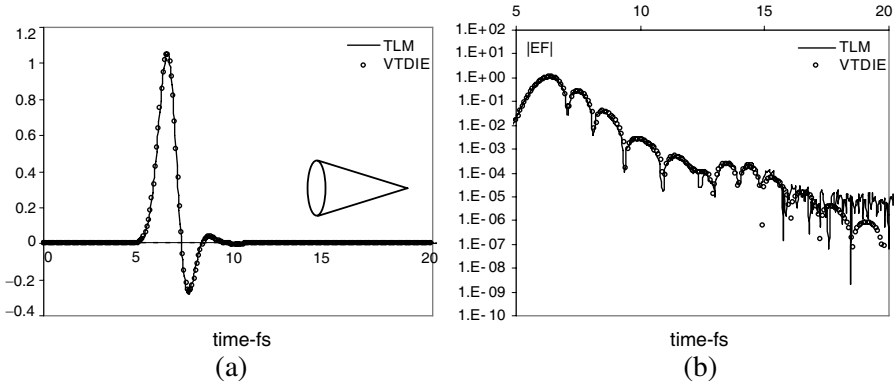

Figure 6. Electric field at the centre of the dielectric cone with base radius $a = 0.25\,\mu\text{m}$ and a height $h = 1.0\,\mu\text{m}$. VTDIE, in circles, and the corresponding TLM results generated form simulating an identical structure and input, in solid line. In both methods, a spatial step size $\Delta x = 0.025$, yielding a total number of elements (cells) $N_e = 4328$ is used. (a) Linear scale. (b) Logarithmic scale.

(cells), $N_e = 10648$, used to populate the dielectric cube. The two sets of results show an excellent agreement. The minor discrepancy between the differential equations based scheme results, in this case TLM, and the Volterra TDIE scheme may be attributed to the

artificial termination of the simulation window with absorbing and/or matching boundary conditions. It is therefore noted that for the TLM scheme and for the specified propagation time in Fig. 3, a simulation window of at least a factor of four of the actual scatterer, V, size is required in order to eliminate any unwanted contribution from reflected signals upon hitting the artificially truncated boundaries, which are unphysical. This dictates the need for additional computational resources; highlighting a significant advantage of the proposed scheme in comparison to differential equations based scheme, and in particular when considering this type of problems where a relatively small discontinuity region is situated in an otherwise uniform background.

For comparison, with emphasis on illustrating the computational resources required for this particular case, when both algorithms are run on the same machine, a PC with an AMD Athlon 2.00 GHz processor; the Volterra TDIE scheme was found to require a 25% less in run-time than that of the TLM method. In addition, the total RAM required for the Volterra TDIE and TLM are 249 MB and 900 MB, respectively. Notwithstanding this, there is a significant scope for increasing the efficiency of the algorithmic development of the TDIE code, which is currently being optimized for this purpose; as well as being extended to operate on parallel computing environments with ease. This promises to offer a further substantial reduction in the computational resources required for the TDIE model when correctly exploited as shall be presented in a separate publication. In addition, exploitation of the already tested fast Fourier transform acceleration technique [12] is currently being considered for this scheme. Next, the transient time-dependent electric field of a dielectric microsphere is considered.

3.2. Accuracy

For further validation of the accuracy and convergence of the proposed Volterra TDIE method; a three-dimensional dielectric problem is considered, where the transient time-dependent field can be analytically determined. A dielectric microsphere of radius $a = 0.5\,\mu$m situated at the centre $r_o = (0\,\mu\text{m},\ 0\,\mu\text{m},\ 0\,\mu\text{m})$ of a right-handed Cartesian coordinate system is therefore studied here, as shown in Fig. 4. The parameters chosen for the incident pulse are $t_o = 2.0\,$fs and $h = 1.85\,$fs. Four spatial step size, $\Delta x(\mu\text{m})$, values of (0.05, 0.04, 0.03, 0.025) are used to generate the results, yielding a total number of elements, $N_e = (4139, 8217, 19304, 33371)$ to discretize the microsphere, respectively, as demonstrated in Fig. 4. It is clear that the smaller the step size; and therefore the more elements used to populate the problem under investigation, the more accurate the

solution obtained. Here, the reference result taken for comparison is that which is analytically generated using the Mie series solution, in dotted line.

Figure 4(a) shows the transient time-dependent response for various Δx, and Fig. 4(b) shows the same set of results on a logarithmic scale, but for a selected duration of time, with emphasis to demonstrate convergence of the algorithm. While a relatively large step size is found to be adequate enough to predict the general response of the problem under investigation, a smaller step size is required for higher accuracy. This is emphasized at the peak amplitude values. Next, the more general cases including a cylinder and a cone are considered.

3.3. General Cases

In this section, dielectric structures whose boundaries are not only curved, for example a cylinder, but also non-tangential to the coordinate axis, such as a cone, are now considered for further validation of the proposed method.

A dielectric cylinder and a cone of base radius $a = 0.25\,\mu\text{m}$ and height $h = 1.0\,\mu\text{m}$, situated at the centre r_o=(0 μm, 0 μm, 0 μm) of a right-handed Cartesian coordinate system is studied, as illustrated in Fig. 5 and Fig. 6, respectively. An identical input signal to the example considered in Fig. 3 is used as the incident field with a spatial step size $\Delta x = 0.025\,\mu\text{m}$. This results in a discretized rectangular mesh within the scatterer, V, of $N_e = 12200$ and $N_e = 4328$ elements, respectively. Again, the two sets of results show excellent agreement. However, the Volterra TDIE scheme seems to better approximate the solution than the TLM counterpart for the case of a cone. This is illustrated in Fig. 6(b), and in particular for the late time response. Discrepancies in this case may be attributed to interaction of the reflected signals from the artificially terminated boundaries with the solution of propagating signal; hence it requires a larger simulation window and therefore more computational resources in order to obtain a cleaner response when using the TLM model.

4. CONCLUSION

A volume time domain integral equation based scheme to analyze the transient time-dependent electric field of dielectric objects has been described. The scheme is demonstrated for the case where rectangular volume elemental building blocks are used to model the geometry of the problem under investigation. This technique has been verified for representative geometries against analytical and time

domain differential equation based scheme solutions illustrating its accuracy and stability. Stability of the proposed scheme is achieved by the application of a low pass FIR filter with constant group delay to the temporal variation of the electric field during the computations, and is implemented at the core of the algorithm. Dielectric bodies only have been studied in this paper, but the method can be readily extended to include other materials with ease. Future work includes generalizing the scheme for plasmas, semiconductors, non-linear and dispersive media with losses. The scheme will also be used to study waveguides containing nanoparticles and structures involving surface plasmonics.

ACKNOWLEDGMENT

The Mie series results presented in this work were provided by Dr Chris Smartt whose assistance and fruitful discussions in this respect are gratefully acknowledged. The authors also acknowledge, with thanks, the financial support of this work from EPSRC under grant reference EP/D068444/1.

REFERENCES

1. Jeong, Y. C. and B. G. Lee, "Characteristics of second-harmonic generation including third-order nonlinear interactions," *IEEE Journal of Quantum Electronics*, Vol. 37, 1292–1300, Oct. 2001.
2. Chi, J. W. D., L. Chao, and M. K. Rao, "Time-domain large-signal investigation on nonlinear interactions between an optical pulse and semiconductor waveguides," *IEEE Journal of Quantum Electronics*, Vol. 37, 1329–1336, Oct. 2001.
3. Moten, K., C. H. Durney, and T. G. Stockham, "Electromagnetic pulsed-wave radiation in spherical-models of dispersive biological substances," *Bioelectromagnetics*, Vol. 12, 319–333, Apr. 1991.
4. Dorn, O., H. Bertete-Aguirre, J. G. Berryman, and G. C. Papanicolaou, "A nonlinear inversion method for 3d electromagnetic imaging using adjoint fields," *Inverse Problems*, Vol. 15, 1523–1558, Dec. 1999.
5. Yee, K. S., "Numerical solution of initial boundary value problems involving maxwells equations in isotropic media," *IEEE Transactions on Antennas and Propagation*, Vol. 14, 302–307, May 1966.
6. Christopoulos, C., *The Transmission Line Modelling Method: TLM*, IEEE Press, 1995.

7. Holland, R., V. P. Cable, and L. C. Wilson, "Finite-volume time-domain (FVTD) techniques for EM scattering," *IEEE Transactions on Electromagnetic Compatibility*, Vol. 33, 281–294, Nov. 1991.
8. Bennett, C. L. and H. Mieras, "Time domain scattering from open thin conducting surfaces," *Radio Science*, Vol. 16, 1231–1239, 1981.
9. Mieras, H. and C. L. Bennett, "Space-time integral-equation approach to dielectric targets," *IEEE Transactions on Antennas and Propagation*, Vol. 30, 2–9, Jan. 1982.
10. Rao, S. M. and D. R. Wilton, "Transient scattering by conducting surfaces of arbitrary shape," *IEEE Transactions on Antennas and Propagation*, Vol. 39, 56–61, Jan. 1991.
11. Ergin, A. A., B. Shanker, and E. Michielssen, "Fast transient analysis of acoustic wave scattering from rigid bodies using a two-level plane wave time domain algorithm," *Journal of the Acoustical Society of America*, Vol. 106, 2405–2416, Nov. 1999.
12. Yilmaz, A. E., J. M. Jin, and D. S. Weile, "A fast fourier transform accelerated marching-on-in-time algorithm for electromagnetic analysis," *Electromagnetics*, Vol. 21, 181–197, Apr. 2001.
13. Rynne, B. P. and P. D. Smith, "Stability of time marching algorithms for the electric-field integral-equation," *Journal of Electromagnetic Waves and Applications*, Vol. 4, No. 12, 1181–1205, 1990.
14. Vechinski, D. A. and S. M. Rao, "A stable procedure to calculate the transient scattering by conducting surfaces of arbitrary shape," *IEEE Transactions on Antennas and Propagation*, Vol. 40, 661–665, Jun. 1992.
15. Sadigh, A. and E. Arvas, "Treating the instabilities in marching-on-in-time method from a different perspective," *IEEE Transactions on Antennas and Propagation*, Vol. 41, 1695–1702, Dec. 1993.
16. Davies, P. J., "A stability analysis of a time marching scheme for the general surface electric field integral equation," *Applied Numerical Mathematics*, Vol. 27, 33–57, May 1998.
17. Manara, G., A. Monorchio, and R. Reggiannini, "A space-time discretization criterion for a stable time-marching solution of the electric field integral equation," *IEEE Transactions on Antennas and Propagation*, Vol. 45, 527–532, Mar. 1997.
18. Bluck, M. J. and S. P. Walker, "Time-domain BIE analysis of large three-dimensional electromagnetic scattering problems,"

IEEE Transactions on Antennas and Propagation, Vol. 45, 894–901, May 1997.

19. Pinello, W., A. Ruehli, and A. Cangellaris, "Stabilization of time domain solutions of EFIE based on partial element equivalent circuit models," *IEEE Antennas and Propagation Society International Symposium 1997*, Vols. 1–4, 966–969, Jul. 1997.
20. Dodson, S., S. P. Walker, and M. J. Bluck, "Implicitness and stability of time domain integral equation scattering analysis," *Applied Computational Electromagnetics Society Journal*, Vol. 13, 291–301, 1998.
21. Rao, S. M. and T. K. Sarkar, "Implicit solution of time-domain integral equations for arbitrarily shaped dielectric bodies," *Microwave and Optical Technology Letters*, Vol. 21, 201–205, May 1999.
22. Sarkar, T. K., W. Lee, and S. M. Rao, "Analysis of transient scattering from composite arbitrarily shaped complex structures," *IEEE Transactions on Antennas and Propagation*, Vol. 48, 1625–1634, Oct. 2000.
23. Vechinski, D. A., S. M. Rao, and T. K. Sarkar, "Transient scattering from 3-Dimensional arbitrarily-shaped dielectric bodies," *Journal of the Optical Society of America*, Vol. 11, 1458–1470, Apr. 1994.
24. Pocock, M. D., M. J. Bluck, and S. P. Walker, "Electromagnetic scattering from 3-D curved dielectric bodies using time-domain integral equations," *IEEE Transactions on Antennas and Propagation*, Vol. 46, 1212–1219, Aug. 1998.
25. Yilmaz, A. E., J. M. Jin, and E. Michielssen, "Time domain adaptive integral method for surface integral equations," *IEEE Transactions on Antennas and Propagation*, Vol. 52, 2692–2708, Oct. 2004.
26. Gres, N. T., A. A. Ergin, E. Michielssen, and B. Shanker, "Volume-integral-equation-based analysis of transient electromagnetic scattering from three-dimensional inhomogeneous dielectric objects," *Radio Science*, Vol. 36, 379–386, May–Jun. 2001.
27. Schaubert, D. H., D. R. Wilton, and A. W. Glisson, "A tetrahedral modeling method for electromagnetic scattering by arbitrarily shaped inhomogeneous dielectric bodies," *IEEE Transactions on Antennas and Propagation*, Vol. 32, 77–85, Jan. 1984.
28. Silvester, P. P. and R. L. Ferrari, *Finite Elements for Electrical Engineers*, Cambridge University Press, Cambridge, UK, 1990.

29. Peterson, A. F., "Analysis of heterogeneous electromagnetic scatterers — Research progress of the past decade," *Proceedings of the IEEE*, Vol. 79, 1431–1441, Oct. 1991.
30. Wilton, D. R., "Review of current status and trends in the use of integral-equations in computational electromagnetics," *Electromagnetics*, Vol. 12, 287–341, Jul.–Dec. 1992.
31. Volakis, J. L., A. Chatterjee, and L. C. Kempel, "Review of the finite-element method for 3-dimensional electromagnetic scattering," *Journal of the Optical Society of America A — Optics Image Science and Vision*, Vol. 11, 1422–1433, Apr. 1994.
32. Kottmann, J. P. and O. J. F. Martin, "Accurate solution of the volume integral equation for high-permittivity scatterers," *IEEE Transactions on Antennas and Propagation*, Vol. 48, 1719–1726, Nov. 2000.
33. Yilmaz, A. E., B. Shanker, J. M. Jin, and E. Michielssen, "Efficient solution of time domain volume integral equations using the adaptive integral method," *Proceedings of the USNC/CNC/URSI Meeting*, 711, Jun. 2003.
34. Harrington, R. F., *Field Computations by Moment Methods*, Macmillan, New York, 1968.
35. Volakis, J. L. and K. Barkeshli, "Applications of the conjugate radient FFT method to radiation and scattering," *Progress In Electromagnetics Research*, Vol. 05, 159–239, 1991.
36. Nerukh, A. G., "Evolutionary approach in transient electrodynamics problems," *Radio Science*, Vol. 30, 481–491, May–Jun. 1995.
37. Nerukh, A. G., I. V. Scherbatko, and O. N. Rybin, "The direct numerical calculation of an integral volterra equation for an electromagnetic signal in a time-varying dissipative medium," *Journal of Electromagnetic Waves and Applications*, Vol. 12, 163–176, 1998.
38. Nerukh, A. G., I. V. Scherbatko, and M. Marciniak, *Electromagnetics of Modulated Media with Applications to Photonics*, Nat. Inst. Telecommun., Warsaw, Poland, 2001.
39. Fedotov, F. V., A. G. Nerukh, T. A. Benson, and P. Sewell, "Investigation of electromagnetic field in a layer with time-varying medium by volterra intergral equation method," *Journal of Lightwave Technology*, Vol. 21, 305–314, Jan. 2003.
40. Al-Jarro, A., P. Sewell, T. M. Benson, and A. Nerukh, "Effective and flexible analysis for propagation in time varying waveguides," *Optical and Quantum Electronics*, Vol. 36, 133–144, Jan.–

Feb. 2004.

41. Benson, T. M., A. Al-Jarro, P. Sewell, V. Janyani, J. D. Paul, and A. Vukovic, "Simulation of nonlinear integrated photonics devices: A comparison of tlm and numerical time domain integral equation approaches," *Ultra-wideband, Short-pulse Electromagnetics*, Vol. 7, 80–88, 2007.
42. Al-Jarro, A., P. Sewell, T. M. Benson, and A. Vukovic, "A volterra integral equation algorithm on triangulated space time meshes," *Proceedings of the 2007 Workshop on Computational Electromagnetics in Time-domain*, 1–4, Perugia, 2007.
43. Al-Jarro, A., P. Sewell, T. M. Benson, and A. Vukovic, "A volterra time-domain integral equation algorithm on unstructured meshes: 3D model," *Proceedings of the 25th International Review of Progress in Applied Computational*, 792–796, Monterey, Mar. 2009.
44. Al-Jarro, A., P. Sewell, T. M. Benson, and A. Vukovic, "Stabilizing 3D volterra time domain integral equation algorithms," *International Symposium on Antennas and Propagation*, Bangkok, Oct. 2009.
45. Sarto, M. S. and A. Scarlatti, "Suppression of late-time instabilities in 3D-FDTD analyses by combining digital filtering techniques and efficient boundary conditions," *IEEE Transactions on Magnetics*, Vol. 37, 3273–3276, Sep. 2001.
46. Waldvogel, J., "Newtonian potential of homogeneous polyhedra," *Journal of Applied Mathematics and Physics*, Vol. 30, 388–398, Mar. 1979.
47. Waldvogel, J., "Newtonian potential of homogeneous cube," *Journal of Applied Mathematics and Physics*, Vol. 27, 867–871, Nov. 1976.
48. Paul, J., C. Christopoulos, and D. W. P. Thomas, "Generalized material models in TLM — Part I: Materials with frequency-dependent properties," *IEEE Transactions on Antennas and Propagation*, Vol. 47, 1528–1534, Oct. 1999.
49. Mie, G., "A contribution to the optics of turbid media: Especially colloidal metal solutions," *Annals of Physics*, Vol. 25, 377–445, 1908.
50. Oppenheim, A. V. and R. W. Schafer, *Discrete-time Signal Processing*, Englewood Cliffs, Prentice Hall, New Jersey, 1989.